Dynamic thermal buckling of spherical porous shells

Talebi, S.; Hedayati, R.; Sadighi, M.; Ashoori, A. R.

DOI
10.1016/j.tws.2021.108737

Publication date
2022

Document Version
Final published version

Published in
Thin-Walled Structures

Thin-Walled Structures 172 (2022) 108737

Contents lists available at ScienceDirect

Thin-Walled Structures

journal homepage: www.elsevier.com/locate/tws

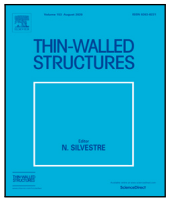

Full length article

Dynamic thermal buckling of spherical porous shells

S. Talebi [a], R. Hedayati [b,*], M. Sadighi [a], A.R. Ashoori [a]

[a] Mechanical Engineering Department, Amirkabir University of Technology, Tehran, Iran
[b] Department of Aerospace Structures and Materials (ASM), Delft University of Technology (TU Delft), Kluyverweg 1, 2629 HS Delft, The Netherlands

ARTICLE INFO

Keywords:
Snap-through instability
Budiansky criterion
Temperature dependency
Ritz–Chebyshev method

ABSTRACT

The aim of present work is to address nonlinear dynamic thermal buckling of shallow spherical functionally graded porous shells subjected to transient thermal loading using the first order shear deformation theory (FSDT). A power-law distribution as well as cosine-type porosity distribution are used to model the variation of constituents through the shell thickness. Thermomechanical properties are assumed to be temperature dependent. Using Crank–Nicolson time marching scheme, an iterative procedure is employed to solve nonlinear transient heat conduction equation. For thermal boundary conditions, the outer surface of shells is kept at a reference temperature, while the inner surface experiences a sudden temperature rise. Geometrical type of nonlinearity in the sense of von-Karman is taken into account. The highly coupled nonlinear governing equations of motion are extracted by constructing the appropriate weak form and also using multi-term Ritz–Chebyshev method. The resulting ODEs are then reduced to a system of nonlinear algebraic equations by employing the well-known Newmark family of time integration schemes. The latter equations are solved by means of Newton–Raphson iteration procedure. Budiansky criterion is used to recognize critical parameters of dynamic instability of shells due to applied thermal shocks. Some comparison studies are conducted in order to verify the accuracy of results of the present work. Moreover, various parametric studies are performed to assess the influence of involved parameters.

1. Introduction

Since the primary work of Boley [1] in 1956, the subject of thermally induced vibrations of solid structures have been pursued in hundreds of publications. Vibrations of beams subjected to simple harmonic oscillation of boundary temperature have been studied by Venkataramana and Jana [2]. Bruch [3] et al. investigated the suppression of vibrations of beam structures induced by thermal loading. Moreover, a general numerical method for thermally induced vibrations of beam structures has been proposed by Manolis and Beskos [4]. Boley and Barber [5] extended the work of Boley [1] on beams to the case of rectangular plates. According to Reissner variational energy principle, Stroud and Mayers [6] studied the behavior of rectangular plates subjected to thermal shocks. Nakajo and Hayashi [7,8] conducted both theoretical and experimental research into the subject of circular plate vibrations under thermal shocks. Generalization to thermally-shocked polygonal plates has been presented by Das [9]. Thermally induced vibrations of laminated plates also studied by Tauchert [10] and Chang et al. [11]. Rapid heating of circular functionally graded plates has been presented by Kiani and Eslami [12]. Geometrical nonlinearity in the sense of von-Karman as well as temperature-dependency of thermomechanical properties were taken into account in their work. The extension of thermally induced vibrations of solid structures to shell geometries is due to Kraus [13]. Huang and Tauchert [14,15] investigated both linear and geometrically nonlinear vibrations of doubly-curved panels due to thermal loads. They demonstrated the remarkable result that a full dynamic analysis leads to snap-through buckling phenomenon. The problem of instability of shells, however, dates from the beginning of the twentieth century.

Using the linear membrane shell theory, the critical values of external pressure were extracted by Zoelly [16]. Critical buckling loads of isotropic shperical shells have been obtained by Karman and Tsien [17] in which nonlinear analysis is employed. A theoretical and experimental research on imperfection sensitivity of spherical shells has been conducted by Wunderlich and Albertin [18]. Combining external pressurizing with uniform thermal loading and employing Galerkin weighted residual method, analysis of isotropic shallow spherical shells has been conducted by Shahsiah and Eslami [19]. Primary studies on dynamic instability of shells dates back to 1960s. Utilizing Galerkin weighted residual method, Budiansky and Roth [20] investigated dynamic instability of spherical shells. The latter research introduced the well-known Budiansky criterion of dynamic buckling: The critical value of involved load parameter is the one at which a small variation of the load parameter results in a remarkable difference in structural

* Corresponding author.
E-mail address: R.hedayati@tudelft.nl (R. Hedayati).

https://doi.org/10.1016/j.tws.2021.108737
Received 23 April 2021; Received in revised form 18 November 2021; Accepted 26 November 2021
Available online xxxx

response. In addition to Budiansky criterion, Simitses [21] also presented a criterion in which the concept of modified total potential energy was introduced. The main advantage of Simitses criterion over Budiansky criterion is that the former employs a time-independent approach, while the latter requires full dynamic analysis of governing equations. The Simitses criterion is not, however, applicable to problems with time-dependent loading. Budiansky criterion has therefore been used extensively over the past decades due to its generality. Dynamic instability analysis of isotropic spherical shells subjected to various loading and boundary conditions has been presented based on different numerical methods [22–24]. An experimental research has been conducted by Lock et al. [23] to validate critical buckling loads of domes. A number of investigations have addressed dynamic snap-through instability of orthotropic spherical shells [25–27].

Researches on dynamic snap-through buckling of spherical functionally graded shells are more limited in number. Ganapathi and Varadan [28] studied the dynamic snap-through instability of externally pressurized spherical FGM shells in which kinematic assumptions are according to first order shear deformation theory and von-Karman geometrical nonlinearity. Prakash et al. [29] investigated the nonlinear dynamic thermal buckling of FGM spherical caps due to a constant field of temperature rise. Axisymmetric snap-through behavior of shallow spherical Piezo-FGM shells under thermo-electro-mechanical loading has been presented by Sabzikar and Eslami [30]. In recent years, functionally graded porous materials (FGPMs) have drawn the attention of investigators due to their potential applications in various systems. Wang and Zu [31] focused on the large amplitude vibration of thin functionally graded plates with porosities happening due to technical issues during preparation. According to first order shear deformation plate theory, Rezaei et al. [32] investigated the free vibration analysis of rectangular FGM plates with porosities. Wang et al. [33] studied the vibrations of longitudinally traveling porous functionally graded plates. Taking into account the geometrical nonlinearity, Wang and Zu [34] conducted a study on the vibrations of rectangular functionally graded plates with porosities and moving in thermal environment. For moving functionally graded materials containing porosities, Wang and Yang [35] presented the nonlinear vibrations of plates coming into contact with incompressible, inviscid and irrotational liquid. Free vibration analysis of light-weight non-uniformly porous plates resting on two parameter elastic foundation has been investigated by Heshmati and Daneshmand [36]. Li et al. [37] studied the static linear elasticity, natural frequency and buckling behavior of porous functionally graded plates based on isogeometric analysis. Novel quasi-3D theories of displacement field for functionally graded porous structures have been proposed by Zenkour [38] and Shahsavari [39]. Nonlinear dynamic buckling analysis of functionally graded plates and shells have been studied by Bich et al. [40] and Li et al. [41], respectively. Employing Chebyshev–Ritz method, Chen et al. [42] investigated the bending and buckling analyses of porous functionally graded plates. For cylindrical shells, Nam et al. [43] presented the buckling and postbuckling of porous shells with functionally graded composite coating subjected to torsion and thermal loading. The buckling and free vibration analysis of cellular porous plates has been investigated by Thang et al. [44] based on the first order shear deformation theory of plates. The buckling and postbuckling behavior of rectangular FGM porous plates have been studied analytically by Cong et al. [45]. Dynamic buckling of thermally shocked porous shells are, however, absent in the literature.

As the literature survey demonstrates, no work, to the best of the authors' knowledge, has been reported on nonlinear dynamic snap-through instability of temperature-dependent spherical functionally graded porous shells subjected to thermal shock. The present study is therefore directed toward filling this gap in the literature. For the latter purpose, Hamilton's principle is utilized to construct nonlinear governing equations of motion and associated boundary conditions. All thermomechanical properties are assumed to be temperature dependent. In order to solve transient heat conduction equation, an iterative scheme consisting of central finite difference and Crank–Nicolson time integration is used. Geometrical nonlinearity in sense of von-Karman as well as first order shear deformation theory are considered as kinematic assumptions. Ritz–Chebyshev method is utilized to spatially discretize nonlinear governing equations of motion. Newmark family of time integration schemes is employed to reduce the governing equations of motion to a system of nonlinear algebraic equations. The latter is solved iteratively using the well-known Newton–Raphson method scheme. The critical parameter of thermal shock resulting in dynamic snap-through instability is recognized by Budiansky criterion. The numerical results of this study are first justified by available data from open literature. Various parametric studies are then presented to investigate the influence of involved parameters.

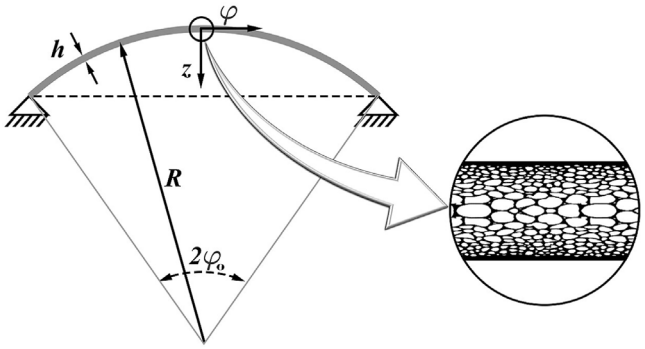

Fig. 1. Schematic configuration of a shallow spherical FGPM shell.

2. Preliminaries

A shallow spherical functionally graded porous shell of radius R, thickness h and angle subtended by the shell span at the center of the sphere $2\varphi_0$ is considered (Fig. 1). As shown, a curvilinear coordinate system (φ, ϑ, z) with its origin located on mid-surface of the shell is considered. The coordinate measured through the shell thickness is considered to be positive radially inward. The inner surface of the shell, being initially at a reference temperature T_0, is subjected to a uniform temperature rise Θ_0. Moreover, mechanical boundary conditions of the shell are considered to be immovable simply-supported. Since thermal loading and boundary conditions are symmetric, axisymmetric response of shallow FGM porous shells with no azimuthal dependence is studied in the present work.

In order to define equivalent thermomechanical properties of FGM porous shells, an appropriate homogenization technique is required. The well-known Voigt rule is commonly used for the latter purpose. According to Voigt rule of mixture for FGMs, thermomechanical properties of FGM porous shells, including Young's modulus E, Poisson's ratio ν, the coefficient of thermal expansion α, thermal conductivity κ, mass density ρ and specific heat capacity c, are considered to be a linear function of constituent volume fractions. Assuming a cosine-type of porosity distribution, a typical temperature-dependent thermomechanical property of FGM porous shells, denoted by P, is therefore expressed as

$$P(z,T) = \left(P_m(T) + \left(P_c(T) - P_m(T)\right)V_c(z)\right)\left(1 - \xi\cos\left(\frac{\pi z}{h}\right)\right) \tag{1}$$

where T stands for temperature measured in Kelvin, ξ denotes porosity index and subscripts m and c represent the properties of metal and ceramic constituents, respectively. Temperature dependency of thermomechanical properties is frequently taken into account using Touloukian model [46]

$$P(T) = P_0(P_{-1}T^{-1} + 1 + P_1T + P_2T^2 + P_3T^3) \tag{2}$$

Following a power law for volume fraction of constituents, ceramic and metal volume fractions are written as [34]

$$V_c = \left(\frac{1}{2} + \frac{z}{h}\right)^k, \qquad V_m = 1 - V_c \tag{3}$$

The non-negative constant k is called power law index.

In the present work, displacement field is represented using first order shear deformation shell theory (FSDT) [37]. According to this theory which is suitable for the thin and moderately thick class of shells, displacement field is expressed as

$$\begin{aligned} u_\varphi(\varphi, z, t) &= u(\varphi, t) + z\psi(\varphi, t) \\ u_z(\varphi, z, t) &= w(\varphi, t) \end{aligned} \tag{4}$$

Here, u and w denote the displacements of a typical point on middle surface in the φ and z directions, respectively. Moreover, ψ represents the transverse normal rotation. Taking into account von-Karman assumptions, the nonzero components of strain tensors are

$$\begin{aligned} \varepsilon_\varphi &= \frac{1}{R}\frac{\partial u_\varphi}{\partial \varphi} - \frac{u_z}{R} + \frac{1}{2R^2}\left(\frac{\partial u_z}{\partial \varphi}\right)^2 \\ \varepsilon_\vartheta &= \frac{\cot\varphi}{R}u_\varphi - \frac{u_z}{R} \\ \gamma_{\varphi z} &= \frac{\partial u_\varphi}{\partial z} + \frac{1}{R}\frac{\partial u_z}{\partial \varphi} \end{aligned} \tag{5}$$

In the above equations, ε_φ and ε_ϑ are polar and azimuthal normal strains, respectively. Furthermore, $\gamma_{\varphi z}$ denotes shear strain.

Within the framework of linear thermoelasticity, constitutive law, after appropriate substitution of Lame constants by the coefficients of plane stress state, takes the following form

$$\begin{Bmatrix} \sigma_\varphi \\ \sigma_\vartheta \\ \tau_{\varphi z} \end{Bmatrix} = \begin{bmatrix} Q_{11} & Q_{12} & 0 \\ Q_{12} & Q_{22} & 0 \\ 0 & 0 & Q_{55} \end{bmatrix} \left(\begin{Bmatrix} \varepsilon_\varphi \\ \varepsilon_\vartheta \\ \gamma_{\varphi z} \end{Bmatrix} - \Theta \begin{Bmatrix} \alpha \\ \alpha \\ 0 \end{Bmatrix} \right) \tag{6}$$

The Q_{ij}'s $(i, j = 1, 2, 5)$, known as material stiffness coefficients, are given by

$$\begin{aligned} Q_{11} = Q_{22} &= \frac{E(z,T)}{1-\nu^2(z,T)}, \quad Q_{12} = \frac{\nu(z,T)E(z,T)}{1-\nu^2(z,T)}, \\ Q_{55} &= \frac{E(z,T)}{2(1+\nu(z,T))} \end{aligned} \tag{7}$$

Moreover, $\Theta = T(z,t) - T_0$ is the field of temperature rise. According to FSDT, stress resultants are related to nonzero components of stress tensor through the following definitions

$$(N_\varphi, N_\vartheta, M_\varphi, M_\vartheta, Q_{\varphi z}) = \int_{-\frac{h}{2}}^{\frac{h}{2}} (\sigma_\varphi, \sigma_\vartheta, z\sigma_\varphi, z\sigma_\vartheta, \tau_{\varphi z})\, dz \tag{8}$$

By substituting Eqs. (5) and (6) into (8), the stress resultants are obtained in terms of mid-plane displacements as

$$\begin{Bmatrix} N_\varphi \\ N_\vartheta \\ M_\varphi \\ M_\vartheta \\ Q_{\varphi z} \end{Bmatrix} = \begin{bmatrix} A_{11} & A_{12} & B_{11} & B_{12} & 0 \\ A_{12} & A_{22} & B_{12} & B_{22} & 0 \\ B_{11} & B_{12} & D_{11} & D_{12} & 0 \\ B_{12} & B_{22} & D_{12} & D_{22} & 0 \\ 0 & 0 & 0 & 0 & A_{55} \end{bmatrix} \begin{Bmatrix} \frac{1}{R}u_{,\varphi} - \frac{w}{R} + \frac{1}{2R^2}w_{,\varphi}^2 \\ \frac{\cot\varphi}{R}u - \frac{w}{R} \\ \frac{1}{R}\psi_{,\varphi} \\ \frac{\cot\varphi}{R}\psi \\ \frac{1}{R}w_{,\varphi} + \psi \end{Bmatrix} - \begin{Bmatrix} N^T \\ N^T \\ M^T \\ M^T \\ 0 \end{Bmatrix} \tag{9}$$

Commas henceforth denote partial differentiation. The stretching, stretching-bending and bending stiffness coefficients are defined as

$$(A_{ij}, B_{ij}, D_{ij}) = \int_{-\frac{h}{2}}^{\frac{h}{2}} Q_{ij}(1, z, z^2)\, dz \tag{10}$$

Furthermore, N^T and M^T are thermal resultants and are given by

$$(N^T, M^T) = \int_{-\frac{h}{2}}^{\frac{h}{2}} (1, z)\frac{E(z,T)\alpha(z,T)}{1-\nu(z,T)}\left(T(z,t) - T_0\right) dz \tag{11}$$

As observed from Eq. (11), the temperature field $T(z,t)$ must be known in order to obtain thermally induced resultants. Since initial conditions, thermal loading and thermal boundary conditions are spherically symmetric, the temperature field T varies only in the radial direction

$$\frac{1}{(R-z)^2}\frac{\partial}{\partial z}\left((R-z)^2\kappa(z,T)\frac{\partial T}{\partial z}\right) = \rho(z,T)\, c(z,T)\frac{\partial T}{\partial t} \tag{12}$$

In the latter equation, the term

$$\frac{1}{(R-z)^2}\,\kappa(z,T)\,\frac{\partial T}{\partial z}\frac{\partial}{\partial z}(R-z)^2$$

is an order of $\frac{h}{R}$ smaller than other terms. Since the thickness of the shell is negligible compared to its radius ($\frac{h}{R} \ll 1$), the above term may be neglected and the heat conduction equation takes the form

$$\frac{\partial}{\partial z}\left(\kappa(z,T)\frac{\partial T}{\partial z}\right) = \rho(z,T)\, c(z,T)\frac{\partial T}{\partial t} \tag{13}$$

The initial condition is given by

$$T(z,0) = T_0 \tag{14}$$

As boundary conditions, the outer surface is kept at a reference temperature T_0, while the inner surface experiences a temperature rise of Θ_0

$$T\left(-\frac{h}{2}, t\right) = T_0, \qquad T\left(\frac{h}{2}, t\right) \equiv T_1 = T_0 + \Theta_0 \tag{15}$$

Eq. (13) should be solved along with conditions (14) and (15) in order to obtain the temperature field. For the latter purpose, a hybrid spatial–temporal discretization is required. By employing second order finite difference discretization in the spatial domain and also Crank–Nicolson scheme as the time marching procedure, the heat conduction equation becomes

$$\mathbf{C}_\mathrm{T}(\mathbf{T})\,\dot{\mathbf{T}} + \mathbf{K}_\mathrm{T}(\mathbf{T})\,\mathbf{T} = \mathbf{F}_\mathrm{T}(\mathbf{T}) \tag{16}$$

As observed, due to temperature dependency of the material properties, the matrices $\mathbf{C}_\mathrm{T}$ and $\mathbf{K}_\mathrm{T}$ as well as the vector $\mathbf{F}_\mathrm{T}$ involved in the above equation are functions of nodal temperatures $\mathbf{T}$. As a consequence, an iterative numerical scheme is required at each time step. For the latter purpose, Newton–Raphson iterative scheme is adopted.

3. Governing equations

Under the assumptions of uncoupled thermoelasticity, the governing equations of motion of shallow spherical functionally graded porous shells may be obtained using Hamilton's principle expressed as

$$\int_{t_1}^{t_2} (\delta U - \delta K)\, dt = 0 \tag{17}$$

where δK is the variation of kinetic energy of FGM porous shells and is written as

$$\begin{aligned} \delta K &= \int_0^{2\pi} d\vartheta \int_0^{\varphi_0} R^2 \sin\varphi\, d\varphi \int_{-\frac{h}{2}}^{\frac{h}{2}} \rho(z)(\dot{u}_\varphi \delta\dot{u}_\varphi + \dot{u}_z\delta\dot{u}_z)\, dz \\ &= -\int_0^{2\pi} d\vartheta \int_0^{\varphi_0} \Big\{ (I_0\ddot{u} + I_1\ddot{\psi})\delta u + I_0\ddot{w}\delta w + (I_1\ddot{u} + I_2\ddot{\psi})\delta\psi \Big\} \\ &\quad \times R^2 \sin\varphi\, d\varphi \end{aligned} \tag{18}$$

where a dot means differentiation with respect to time. The inertia coefficient I_i is defined as

$$I_i = \int_{-\frac{h}{2}}^{\frac{h}{2}} z^i \rho(z)\, dz \qquad (i = 0, 1, 2) \tag{19}$$

The total virtual strain energy of FGM porous shells due to the nonzero components of stress tensor reads

$$\begin{aligned}\delta U &= \int_0^{2\pi} d\vartheta \int_0^{\varphi_0} R^2 \sin\varphi \, d\varphi \int_{-\frac{h}{2}}^{\frac{h}{2}} (\sigma_\varphi \delta\varepsilon_\varphi + \sigma_\vartheta \delta\varepsilon_\vartheta + \tau_{\varphi z}\delta\gamma_{\varphi z})\, dz \\ &= \int_0^{2\pi} d\vartheta \int_0^{\varphi_0} \Big\{ N_\varphi \Big(\frac{\delta u_{,\varphi}}{R} - \frac{\delta w}{R} + \frac{w_{,\varphi}}{R^2}\delta w_{,\varphi} \Big) + M_\varphi \frac{\delta\psi_{,\varphi}}{R} \\ &\quad + N_\vartheta \Big(\frac{\cot\varphi}{R}\delta u - \frac{\delta w}{R} \Big) + M_\vartheta \frac{\cot\varphi}{R}\delta\psi + Q_{\varphi z}\Big(\frac{\delta w_{,\varphi}}{R} + \delta\psi \Big) \Big\} \\ &\quad \times R^2 \sin\varphi \, d\varphi \end{aligned} \tag{20}$$

Substituting Eqs. (9) into the previous relation and then combining the latter and virtual kinetic energy relation (18) with Hamilton's principle (17) lead to the weak form of governing equations of motion

$$\begin{aligned}&\int_0^{\varphi_0} \sin\varphi \, d\varphi \Big\{ \frac{A_{11}}{R^2}\big(u_{,\varphi}\delta u_{,\varphi} + \cot^2\varphi \, u\delta u\big) + \frac{A_{12}}{R^2}\cot\varphi \, \big(u_{,\varphi}\delta u + u\delta u_{,\varphi}\big) \\ &- \frac{A_{11}+A_{12}}{R^2}\big(w\delta u_{,\varphi} + \cot\varphi \, w\delta u\big) + \frac{A_{11}}{2R^3}w_{,\varphi}^2\delta u_{,\varphi} + \frac{A_{12}}{2R^3}\cot\varphi \, w_{,\varphi}^2\delta u \\ &+ \frac{B_{11}}{R^2}\big(\psi_{,\varphi}\delta u_{,\varphi} + \cot^2\varphi \, \psi\delta u\big) + \frac{B_{12}}{R^2}\cot\varphi \, \big(\psi_{,\varphi}\delta u + \psi\delta u_{,\varphi}\big) \\ &- \frac{A_{11}+A_{12}}{R^2}\big(u_{,\varphi} + \cot\varphi \, u\big)\delta w + \frac{A_{11}}{R^3}u_{,\varphi}w_{,\varphi}\delta w_{,\varphi} + \frac{A_{12}}{R^3}\cot\varphi \, uw_{,\varphi}\delta w_{,\varphi} \\ &+ \frac{A_{11}+A_{12}}{R^2}2w\delta w + \frac{A_{55}}{R^2}w_{,\varphi}\delta w_{,\varphi} - \frac{A_{11}+A_{12}}{2R^3}w_{,\varphi}^2\delta w - \frac{A_{11}+A_{12}}{R^3}ww_{,\varphi}\delta w_{,\varphi} \\ &+ \frac{A_{11}}{2R^4}w_{,\varphi}^3\delta w_{,\varphi} - \frac{B_{11}+B_{12}}{R^2}\big(\psi_{,\varphi} + \cot\varphi \, \psi\big)\delta w + \frac{A_{55}}{R}\psi\delta w_{,\varphi} \\ &+ \frac{B_{11}}{R^3}w_{,\varphi}\psi_{,\varphi}\delta w_{,\varphi} + \frac{B_{12}}{R^3}\cot\varphi \, w_{,\varphi}\psi\delta w_{,\varphi} + \frac{B_{11}}{R^2}\big(u_{,\varphi}\delta\psi_{,\varphi} + \cot^2\varphi \, u\delta\psi\big) \\ &+ \frac{B_{12}}{R^2}\cot\varphi \, \big(u_{,\varphi}\delta\psi + u\delta\psi_{,\varphi}\big) - \frac{B_{11}+B_{12}}{R^2}\big(w\delta\psi_{,\varphi} + \cot\varphi \, w\delta\psi\big) \\ &+ \frac{A_{55}}{R}w_{,\varphi}\delta\psi + \frac{B_{11}}{2R^3}w_{,\varphi}^2\delta\psi_{,\varphi} + \frac{B_{12}}{2R^3}\cot\varphi \, w_{,\varphi}^2\delta\psi + A_{55}\psi\delta\psi \\ &+ \frac{D_{11}}{R^2}\big(\psi_{,\varphi}\delta\psi_{,\varphi} + \cot^2\varphi \, \psi\delta\psi\big) + \frac{D_{12}}{R^2}\cot\varphi \, \big(\psi_{,\varphi}\delta\psi + \psi\delta\psi_{,\varphi}\big) \\ &+ \big(I_0\ddot{u} + I_1\ddot{\psi}\big)\delta u + I_0\ddot{w}\delta w + \big(I_1\ddot{u} + I_2\ddot{\psi}\big)\delta\psi - \frac{N^T}{R^2}w_{,\varphi}\delta w_{,\varphi} \\ &- \frac{N^T}{R}\big(\delta u_{,\varphi} + \cot\varphi \, \delta u\big) + \frac{2N^T}{R}\delta w - \frac{M^T}{R}\big(\delta\psi_{,\varphi} + \cot\varphi \, \delta\psi\big)\Big\} = 0 \end{aligned} \tag{21}$$

Using some integration by parts, the following governing equations of motion are obtained

$$\begin{aligned}&A_{11}(u_{,\varphi\varphi} + \cot\varphi \, u_{,\varphi}) - (A_{11}\cot^2\varphi + A_{12})\, u - (A_{11}+A_{12})\, w_{,\varphi} + A_{11}R^{-1}w_{,\varphi}w_{,\varphi\varphi} \\ &+ (2R)^{-1}(A_{11}-A_{12})\cot\varphi \, w_{,\varphi}^2 + B_{11}(\psi_{,\varphi\varphi} + \cot\varphi \, \psi_{,\varphi}) \\ &- (B_{11}\cot^2\varphi + B_{12})\, \psi = R^2(I_0\ddot{u} + I_1\ddot{\psi}) \end{aligned} \tag{22a}$$

$$\begin{aligned}&R(A_{11}+A_{12})(u_{,\varphi} + \cot\varphi \, u) + (A_{11}+A_{12})\cot\varphi \, u_{,\varphi}w_{,\varphi} + A_{11}(u_{,\varphi\varphi}w_{,\varphi} \\ &+ u_{,\varphi}w_{,\varphi\varphi}) \\ &+ A_{12}(\cot\varphi \, uw_{,\varphi\varphi} - uw_{,\varphi}) + R(A_{55} - N^T)(w_{,\varphi\varphi} + \cot\varphi \, w_{,\varphi}) \\ &- 2R(A_{11}+A_{12})\, w \\ &- (A_{11}+A_{12})(\cot\varphi \, ww_{,\varphi} + ww_{,\varphi\varphi} + 0.5w_{,\varphi}^2) + R^{-1}A_{11}(1.5\, w_{,\varphi}^2 w_{,\varphi\varphi} \\ &+ 0.5\cot\varphi \, w_{,\varphi}^3) \\ &+ R(RA_{55} + B_{11} + B_{12})(\psi_{,\varphi} + \cot\varphi \, \psi) + B_{11}(w_{,\varphi\varphi}\psi_{,\varphi} + w_{,\varphi}\psi_{,\varphi\varphi}) \\ &+ B_{12}(\cot\varphi \, w_{,\varphi\varphi}\psi - w_{,\varphi}\psi) \\ &+ (B_{11}+B_{12})\cot\varphi \, w_{,\varphi}\psi_{,\varphi} - 2R^2N^T = R^3I_0\ddot{w} \end{aligned} \tag{22b}$$

$$\begin{aligned}&B_{11}(u_{,\varphi\varphi} + \cot\varphi \, u_{,\varphi}) - (B_{11}\cot^2\varphi + B_{12})\, u - (RA_{55} + B_{11} + B_{12})w_{,\varphi} \\ &+ R^{-1}B_{11}w_{,\varphi}w_{,\varphi\varphi} \\ &+ (2R)^{-1}(B_{11} - B_{12})\cot\varphi \, w_{,\varphi}^2 + D_{11}(\psi_{,\varphi\varphi} + \cot\varphi \, \psi_{,\varphi}) \\ &- (D_{11}\cot^2\varphi + D_{12})\, \psi \\ &- R^2A_{55}\psi = R^2(I_1\ddot{u} + I_2\ddot{\psi}) \end{aligned} \tag{22c}$$

The associated boundary conditions for immovable simply-supported shells read

$$\begin{aligned}&\varphi = 0: && u = 0, && V_\varphi = 0, && \psi = 0 \\ &\varphi = \varphi_0: && u = 0, && w = 0, && M_\varphi = 0 \end{aligned} \tag{22d}$$

where $V_\varphi = Q_{\varphi z} + R^{-1}N_\varphi w_{,\varphi}$. Furthermore, FGM porous shells are assumed to be initially at rest. This means that

$$\begin{aligned}&u(\varphi,0) = 0, && w(\varphi,0) = 0, && \psi(\varphi,0) = 0 \\ &\frac{\partial u}{\partial t}(\varphi,0) = 0, && \frac{\partial w}{\partial t}(\varphi,0) = 0, && \frac{\partial\psi}{\partial t}(\varphi,0) = 0 \end{aligned} \tag{22e}$$

4. Solution procedure

In order to solve the highly coupled nonlinear equations presented in Eqs. (22a)–(22c) along with boundary conditions (22d) and initial conditions (22e), a spatial discretization scheme is first applied. In the present work, Ritz–Chebyshev method is adopted for the latter purpose. Accordingly, primary variables are approximated as

$$\begin{Bmatrix} u(\varphi,t) \\ w(\varphi,t) \\ \psi(\varphi,t) \end{Bmatrix} = \sum_m \begin{bmatrix} f_m^u(\varphi) & 0 & 0 \\ 0 & f_m^w(\varphi) & 0 \\ 0 & 0 & f_m^\psi(\varphi) \end{bmatrix} \begin{Bmatrix} U_m(t) \\ W_m(t) \\ \Psi_m(t) \end{Bmatrix} \tag{23}$$

Here, f_m^u, f_m^w are f_m^ψ are approximation functions and must satisfy essential type of boundary conditions. Hence

$$\begin{Bmatrix} f_m^u(\varphi) \\ f_m^w(\varphi) \\ f_m^\psi(\varphi) \end{Bmatrix} = \begin{Bmatrix} A^u(\varphi) \\ A^w(\varphi) \\ A^\psi(\varphi) \end{Bmatrix} \mathrm{T}_m\Big(\frac{2\varphi}{\varphi_0} - 1\Big) \tag{24}$$

where T_m stands for Chebyshev polynomials of the first kind, defined as

$$\cos(m\theta) = \mathrm{T}_m(\cos\theta) \tag{25}$$

$A^u(\varphi)$, $A^w(\varphi)$ and $A^\psi(\varphi)$ are also auxiliary functions defined corresponding to essential boundary conditions:

$$\begin{aligned}A^u(\varphi) &= \frac{\varphi}{\varphi_0}\Big(1 - \frac{\varphi}{\varphi_0}\Big) \\ A^w(\varphi) &= 1 - \frac{\varphi}{\varphi_0} \\ A^\psi(\varphi) &= \frac{\varphi}{\varphi_0} \end{aligned} \tag{26}$$

Insertion of the approximation (23) into the weak form presented in Eqs. (21) leads to the spatially discretized form of governing equations as

$$\mathbf{M}(\mathbf{T})\,\ddot{\mathbf{X}} + \mathbf{K}(\mathbf{T},\mathbf{X})\,\mathbf{X} = \mathbf{F}(\mathbf{T}) \tag{27}$$

Here, $\mathbf{M}$ and $\mathbf{K}$ denote the mass and stiffness matrices, respectively. Moreover, $\mathbf{F}$ is the force vector induced by thermal loading. Since geometrical nonlinearity is taken into account, the stiffness matrix $\mathbf{K}$ is a nonlinear function of time-dependent unknown vector $\mathbf{X}$. It is observed that due to temperature dependency of thermomechanical properties, the matrices involved in (27) are also functions of time-dependent temperature vector $\mathbf{T}$. In order to reduce the system of ODEs presented in (27) to a system of nonlinear algebraic equations, the well-known Newmark family of time integration schemes is employed. Applying the constant-average acceleration scheme ($\beta = 0.25$) of Newmark family leads to

$$\hat{\mathbf{K}}(\mathbf{T},\mathbf{X})\,\mathbf{X} = \hat{\mathbf{F}}(\mathbf{T}) \tag{28}$$

where

$$\begin{aligned}\hat{\mathbf{K}}(\mathbf{T},\mathbf{X}) &= \mathbf{K}(\mathbf{T},\mathbf{X}) + \frac{1}{\beta\Delta t^2}\mathbf{M}(\mathbf{T}) \\ \hat{\mathbf{F}}(\mathbf{T}) &= \mathbf{F}(\mathbf{T}) + \mathbf{M}(\mathbf{T})\Big(\frac{1}{\beta\Delta t^2}\mathbf{X} + \frac{1}{\beta\Delta t}\dot{\mathbf{X}} + \frac{1-2\beta}{2\beta}\ddot{\mathbf{X}}\Big) \end{aligned} \tag{29}$$

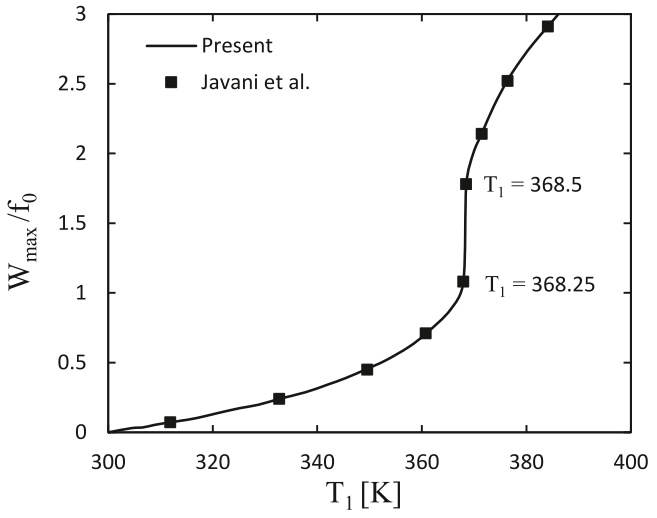

Fig. 2. A comparison of the maximum dimensionless midspan deflection of an isotropic homogeneous spherical shell ($\lambda = 1.7$ and $\mu = 150$) subjected to a sudden temperature rise at the inner surface with the results provided by Javani et al. [24].

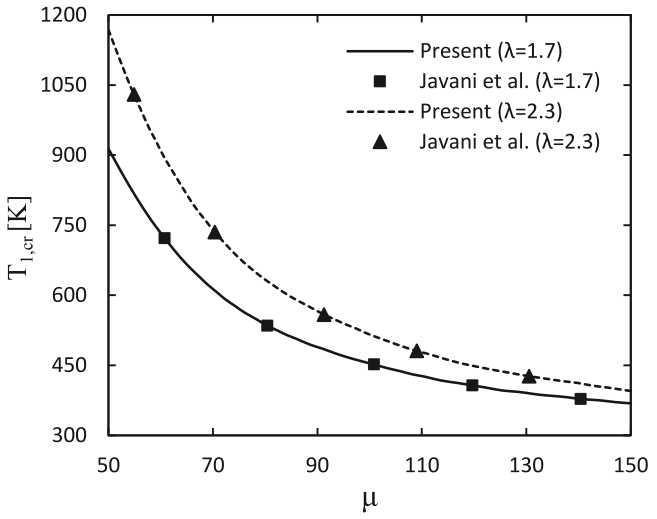

Fig. 3. A comparison of critical temperature of rapidly-heated isotropic homogeneous spherical shells for various values of μ and λ parameters with the results provided by Javani et al. [24].

In order to solve the system of nonlinear algebraic Eqs. (28), an iterative procedure is required. Similar to the case of solving heat conduction equation, Newton–Raphson iterative scheme is adopted for the latter purpose.

5. Results and discussions

The procedure outlined in the previous sections is implemented here to investigate the nonlinear dynamic snap-through instability of temperature-dependent spherical FGM porous shells subjected to transient thermal loading. It is henceforth assumed that W denotes the midspan deflection of shells. For the purpose of greater clarity, W is nondimensionalized by the cap height $f_0 = R(1 - \cos\varphi_0)$. Moreover, $h = 1$ mm is considered unless otherwise stated.

In order to verify numerical results of the present work, a comparison study is first presented to assure the accuracy of solution method. For this purpose, the work by Javani et al. [24] is considered. This research treats dynamic snap-through phenomenon of isotropic shallow spherical caps under transient type of thermal loading. The inner surface of shells is subjected to sudden temperature rise, while the outer surface is kept at a reference temperature. The mechanical boundary conditions are considered to be immovable simply supported. Motion equations are discretized within the shell domain by means of the harmonic differential quadrature method (HDQM). Newmark family of time integration schemes is used to reduce the nonlinear ODEs to a system of nonlinear algebraic equations. Javani et al. [24] also introduced the geometrical parameter λ and slenderness ratio μ as follows

$$\lambda = \sqrt{12}\frac{R\varphi_0^2}{h}, \qquad \mu = 2\sqrt{12}\frac{R\varphi_0}{h} \tag{30}$$

The thermomechanical properties of shells are assumed to be temperature independent and are: $E = 207.79$ GPa, $\nu = 0.3178$, $\alpha = 15.321 \times 10^{-6}$ 1/K, $\kappa = 12.1429$ W/mK, $\rho = 8166$ kg/m^3 and $c = 390.035$ J/kgK. Moreover, the shell thickness is considered to be $h = 1$ mm. Fig. 2 depicts a comparison of the maximum dimensionless midspan deflection of an isotropic homogeneous spherical shell subjected to a sudden temperature rise at the inner surface. In this figure, for any specified value of the inner surface temperature T_1, dynamic response of shells are extracted. The maximum midspan deflection of shells, undimensionalized by the cap height f_0, are then determined. The geometrical parameter and slenderness ratio are selected to be $\lambda = 1.7$ and $\mu = 150$, respectively. For temperatures lower than $T = 368.25$ K, a small positive variation of inner surface temperature is followed by a small increase in the maximum dimensionless midspan deflection. At the temperature $T = 368.25$ K, however, as slight growth of temperature as 0.25 K leads to a rapid increase in the maximum dimensionless midspan deflection. $T = 368.25$ K is therefore recognized as the critical temperature of snap-through buckling according to Budiansky criterion. A comparison on critical temperature of dynamic buckling of shells for a wide range of slenderness ratio μ and also two values of geometrical parameter λ is observed in Fig. 3. As seen, the critical temperature of dynamic snap-through is a strictly increasing function of the geometrical parameter λ. On the other hand, an increase in slenderness ratio reduces the critical temperature of dynamic buckling. As observed, the results of the present study are in good agreement with those reported by Javani et al. [24]. Compared to the work of Javani et al. [24], structures herein are considered to be inhomogeneous and hence the governing equations of motion are more general and complicated. Moreover, porosity is included. Since all thermomechanical properties are assumed to be temperature dependent, heat conduction equation is nonlinear and numerical schemes are inevitable.

After verifying the numerical results of the present work, various parametric studies are conducted to assess the influence of several involved parameters. To this end, ceramic–metal functionally graded material porous shells composed of silicon nitride (Si_3N_4) as the ceramic constituent and stainless steel (SUS304) as the metal constituent are considered in the rest. The inner surface of shells is assumed to be zirconia rich, while the outer one is aluminum rich. It is assumed that FGM porous shells experience Cauchy-type of thermal boundary conditions such that the inner surface of shells is suddenly exposed to a temperature rise, while the outer surface remains at a reference temperature. Thermomechanical properties of silicon nitride and stainless steel (SUS304) are significantly temperature-dependent. This dependency is best described by Touloukian model given by Eq. (2). Corresponding to each thermomechanical property, the P_i coefficients presented in Touloukian model are tabulated in Table 1. In the subsequent numerical results, the shell thickness is discretized using a mesh consisting of 50 nodes. Moreover, the reference temperature is considered to be $T_0 = 300$ K.

In the first example, a spherical linearly graded shell ($k = 1$ and $\xi = 0$) with the geometrical parameter $\lambda = 1.7$ and slenderness ratio $\mu = 150$ is selected. In order to recognize critical temperature of

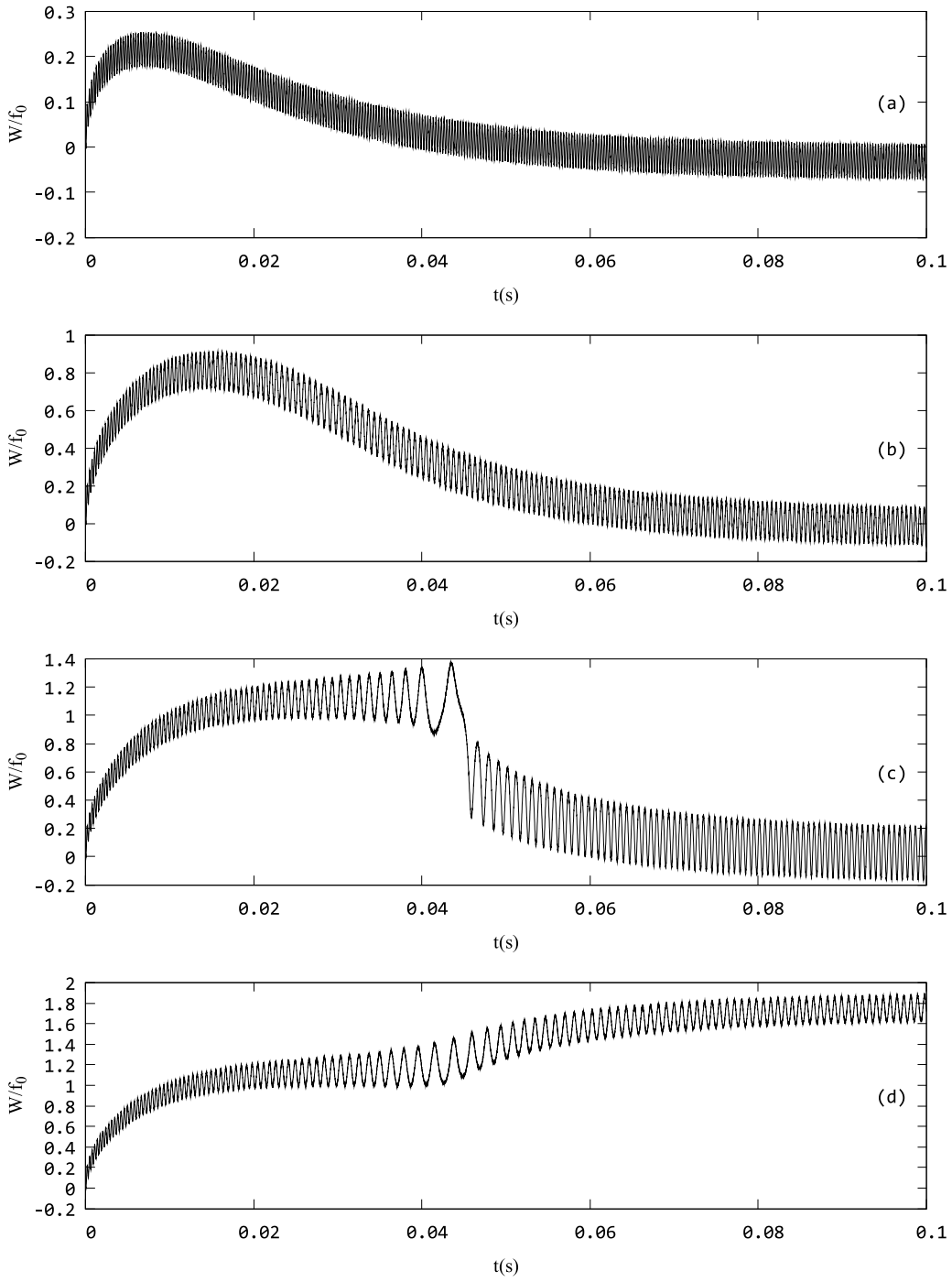

Fig. 4. Temporal evolution of the dimensionless midspan deflection of a spherical linearly graded shell (μ = 150, λ = 1.7 and ξ = 0) for different values of surface temperature rise. (a): T_1 = 350 K, (b): T_1 = 400 K, (c): T_1 = 406.2 K, (d): T_1 = 406.3 K.

dynamic snap-through instability, temporal evolution of the midspan deflection of the shell is required. In Fig. 4, the dimensionless midspan deflection of the shell is plotted versus time (in seconds) for different boundary temperatures. In plots (a) to (d), the values of inner surface temperature are T_1 = 350 K, T_1 = 400 K, T_1 = 406.2 K and T_1 = 406.3 K, respectively. If inertia terms in the governing Eqs. (22a)–(22c) are neglected, thermally induced vibrations observed in Fig. 4 disappear. The latter approach in uncoupled thermoelasticity is known as quasi-static analysis. The curves plotted in Fig. 4 are indeed oscillation around the corresponding quasi-static-analysis curves. Prior to Boley [1], the dominant approach in uncoupled thermoelasticity was quasi-static analysis. Boley [1] demonstrated, however, that although quasi-static analysis is appropriate in many cases, it is inadequate in general. The problem of dynamic snap-through instability is an example of such a case. A quasi-static analysis is not capable of tracing dynamic snap-through buckling. It is observed in Fig. 4 that for temperatures smaller than T = 406.2 K, a small positive change in inner surface temperature results in a slight increase in the maximum dimensionless midspan deflection. At the temperature T = 406.2 K, however, a slight growth of temperature

Table 1
The coefficients of temperature dependency for SUS304 and Si_3N_4 [47].

Material	Property	P_{-1}	P_0	P_1	P_2	P_3
SUS304	E (GPa)	0	201.04	3.079×10^{-4}	-6.534×10^{-7}	0
	ν	0	0.3262	-2.002×10^{-4}	3.797×10^{-7}	0
	α (10^{-6}/K)	0	12.33	8.086×10^{-4}	0	0
	ρ (kg/m^3)	0	8166	0	0	0
	κ (W/mK)	0	15.379	-1.264×10^{-3}	2.092×10^{-6}	-7.223×10^{-10}
	c_v (J/kgK)	0	496.56	-1.151×10^{-3}	1.636×10^{-6}	-5.863×10^{-10}
Si_3N_4	E (GPa)	0	348.43	-3.07×10^{-4}	2.16×10^{-7}	-8.946×10^{-11}
	ν	0	0.24	0	0	0
	α (10^{-6}/K)	0	5.8723	9.095×10^{-4}	0	0
	ρ (kg/m^3)	0	2370	0	0	0
	κ (W/mK)	0	13.723	-1.032×10^{-3}	5.466×10^{-7}	-7.876×10^{-11}
	c_v (J/kgK)	0	555.11	1.016×10^{-3}	2.92×10^{-7}	-1.67×10^{-10}

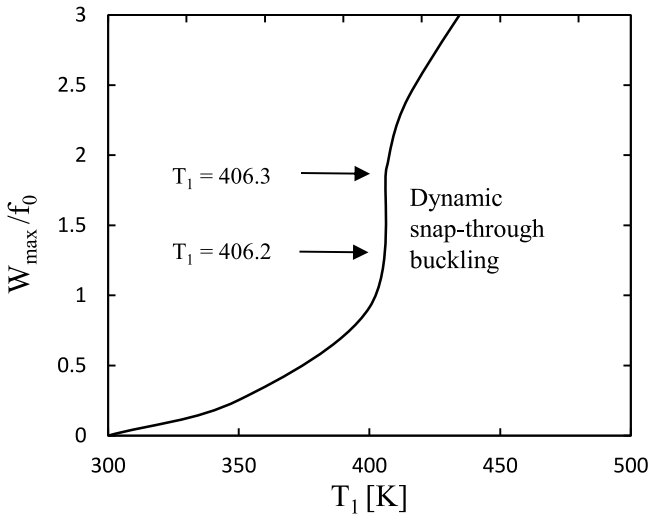

Fig. 5. Maximum dimensionless midspan deflection of a spherical linearly graded shell ($\mu = 150$, $\lambda = 1.7$ and $\xi = 0$) versus the inner surface temperature.

(0.1 K) is followed by a rapid increase in the maximum dimensionless midspan deflection. The temperature $T = 406.2$ K is therefore recognized as the critical temperature of dynamic snap-through instability according to Budiansky criterion. Similar to curves presented in Fig. 4, temporal evolution of the dimensionless midspan deflection of the shell is obtained for various inner surface temperature. Maximum values of the dimensionless midspan deflection are selected for each case of thermal loading and then plotted against inner surface temperature T_1, as shown in Fig. 5. According to Budiansky criterion, the inner surface temperature $T_1 = 406.2$ K is recognized once again as the critical temperature of dynamic snap-through buckling.

The next example is devoted to the study of porosity index influence on the dynamic response of spherical FGM porous shells subjected to surface rapid heating. As before, a spherical linearly graded porous shell ($k = 1$) with the porosity index $\xi = 0.1$, the geometrical parameter $\lambda = 1.7$ and slenderness ratio $\mu = 150$ are selected. Four different values of inner surface temperature are considered: (a) $T_1 = 350$ K, (b) $T_1 = 400$ K, (c) $T_1 = 403.5$ K and (d) $T_1 = 403.6$ K. Temporal evolution of the midspan deflection of the shell is plotted versus time (in seconds) for the aforementioned values of inner surface temperature in Fig. 6. It is observed that a temperature increase as small as 0.1 K in the inner surface temperature results in a significant change of temporal evolution of the dimensionless midspan deflection. Comparing Fig. 6 with Fig. 4, it should be noted that porosity distribution postpones the onset of dynamic snap-through buckling due to thermal shocks. Moreover, porosity inclusion reduces the intensity of dynamic buckling of FGM porous shells subjected to rapid surface temperature rise. Similar to the previous case, maximum values of the dimensionless midspan deflection are selected for each case of thermal loading and then plotted against the inner surface temperature T_1, as shown in Fig. 7. It is again observed that a temperature increase of only 0.1 K in the inner surface temperature leads to a drastic change of temporal evolution of the dimensionless midspan deflection. The inner surface temperature $T_1 = 403.5$ K is therefore recognized as the critical temperature of dynamic buckling according to Budiansky criterion.

Fig. 8 depicts the dynamic snap-through temperature of linearly graded porous shells for different values of porosity index versus slenderness ratio. Three different values of porosity index are considered: $\xi = 0.1$, $\xi = 0.2$ and $\xi = 0.5$. It is seen that the dynamic snap-through temperature is an increasing function of the porosity index. As the slenderness ratio becomes greater, the difference between dynamic buckling temperature for various porosity indices reduces.

The aim of the next study is to investigate the influence of temperature dependency of thermomechanical properties. Fig. 9 shows the dynamic buckling temperature of a linearly graded porous shell for two different cases. In the first case, thermomechanical properties of the porous shell are assumed to be temperature dependent (TD) and to obey Touloukian model given by Eq. (2). In the second case, on the other hand, thermomechanical properties of the shell are assumed to be temperature independent (TID). For the latter purpose, the thermomechanical properties of the shell are evaluated at the reference temperature $T_0 = 300$ K. As observed, the dynamic buckling temperature of the shell increases when the assumption of temperature dependency is incorporated. The influence of power law index on dynamic buckling temperature of functionally graded porous shells is illustrated in Fig. 10. As seen, the dynamic snap-through temperature increases as power law index decreases. This is simply understood since greater values of the power law index leads to a higher equivalent elastic modulus. This in turn implies that dynamic buckling temperature increases. Fig. 11 depicts the dynamic snap-through temperature of linearly graded porous shells versus slenderness ratio. Four different values of geometrical parameter are considered: $\lambda = 1.6$, $\lambda = 1.8$, $\lambda = 2$, $\lambda = 2.2$. It is easily observed that the dynamic snap-through temperature is an increasing function of the geometrical parameter. As the slenderness ratio becomes greater, the difference between dynamic buckling temperature for various geometrical parameters diminishes.

6. Conclusion

Based on the assumptions of von-Karman geometrical nonlinearity and temperature dependency of thermomechanical properties, the nonlinear governing equations of motion of spherical FGM porous shells subjected to thermal shock are derived. The inner surfaces of the shells are kept at a reference temperature, while the outer surfaces

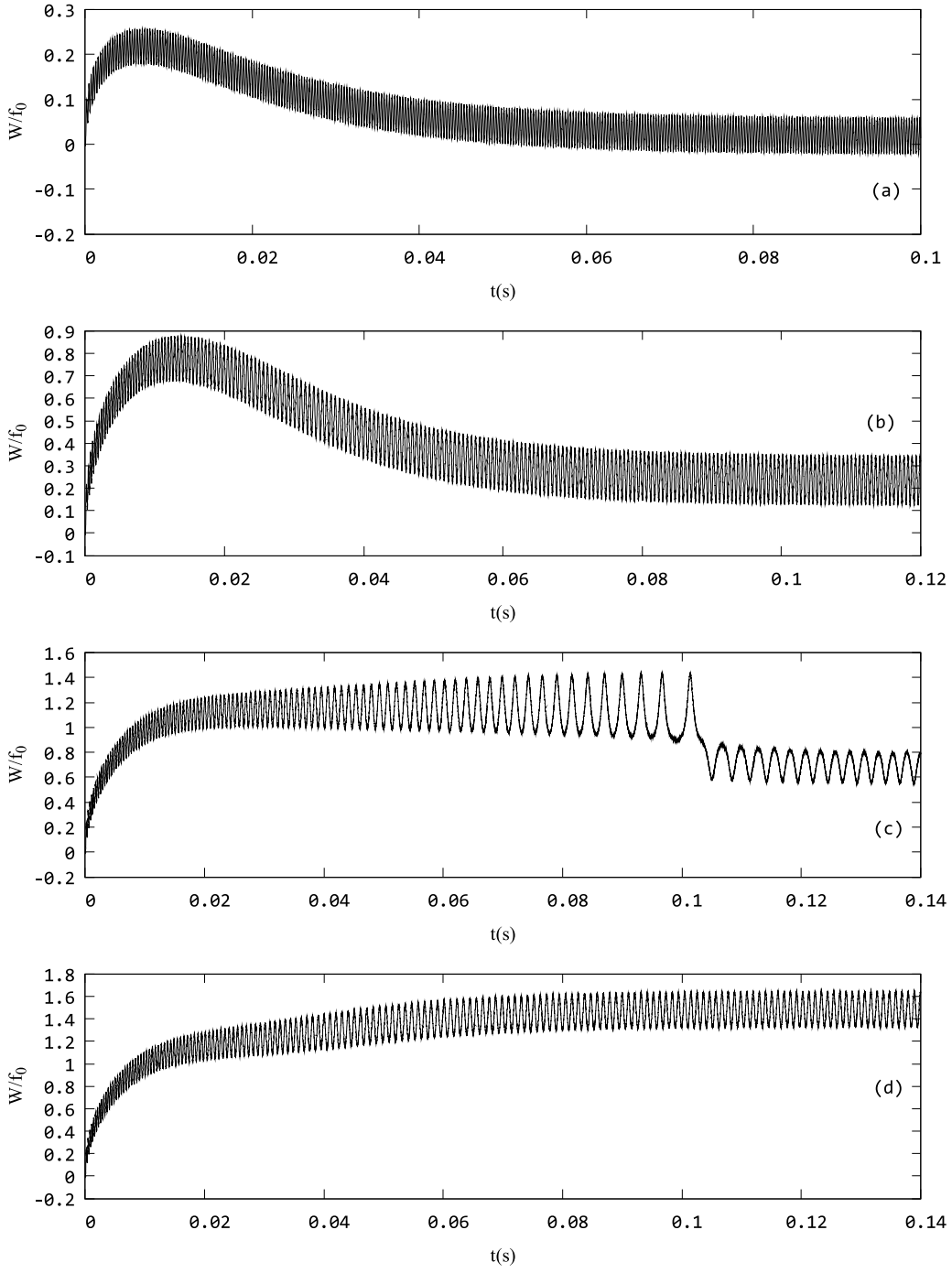

Fig. 6. Temporal evolution of the dimensionless midspan deflection of a spherical linearly graded porous shell (μ = 150, λ = 1.7 and ξ = 0.1) for different values of surface temperature rise. (a): T_1 = 350 K, (b): T_1 = 400 K, (c): T_1 = 403.5 K, (d): T_1 = 403.6 K.

of the shells experience a sudden temperature rise. Employing Ritz–Chebyshev as well as Newmark family of time integration schemes, a system of nonlinear algebraic equations are obtained. The equations are then solved via Newton–Raphson iterative method. Critical boundary temperatures resulting in dynamic snap-through phenomenon are recognized using the well-known Budiansky criterion. The numerical results demonstrate that for the constituents considered herein, dynamic buckling temperature is a decreasing function of porosity index as well as power law index. The geometrical parameter of the shells is also an influential parameter on the critical temperature of shells such that higher values of the geometrical parameter lead to greater dynamic buckling temperatures. The other influential parameter on the critical temperature of the shells is the slenderness ratio. In contrast to the geometrical parameter, critical temperature is a decreasing function of slenderness ratio. Moreover, comparison study on temperature dependency of thermomechanical properties shows that ignoring temperature dependency leads to an underestimated temperature of dynamic snap-through buckling.

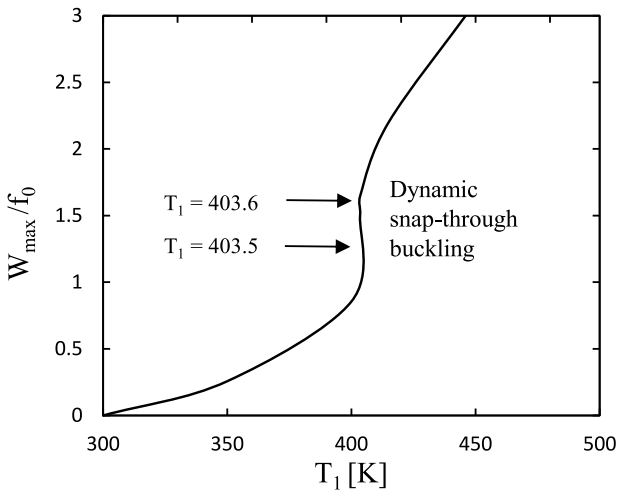

Fig. 7. Maximum dimensionless midspan deflection of a spherical linearly graded porous shell ($\mu = 150$, $\lambda = 1.7$ and $\xi = 0.1$) versus the inner surface temperature.

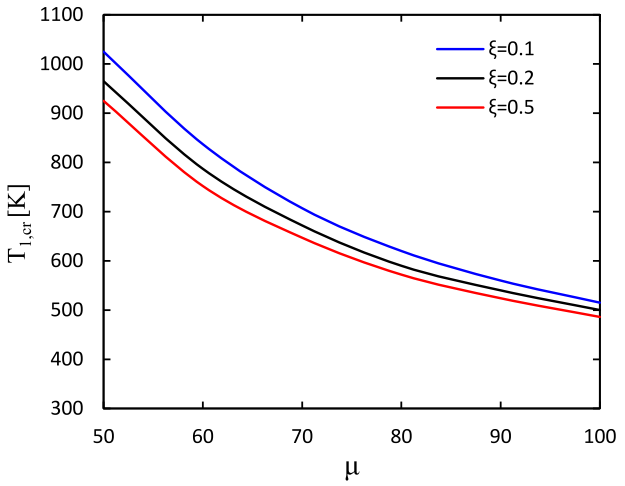

Fig. 8. Dynamic snap-through temperature of spherical linearly graded porous shells ($\lambda = 1.7$) for various porosity indices versus slenderness ratio.

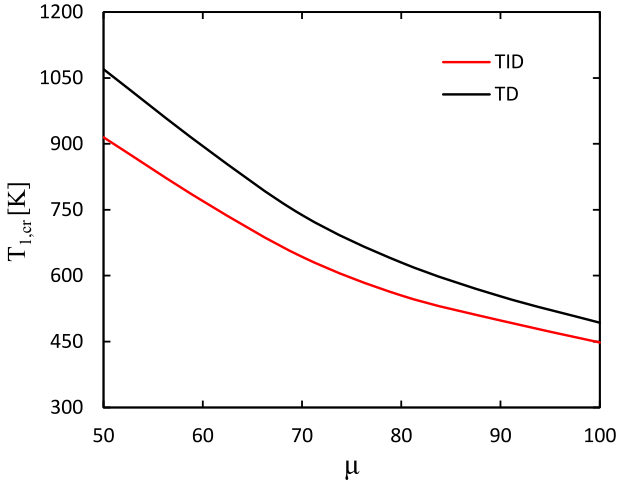

Fig. 9. Dynamic buckling temperature of spherical linearly graded porous shells ($\lambda = 1.7$ and $\xi = 0.1$) for temperature-dependent (TD) and temperature-independent (TID) thermomechanical properties versus slenderness ratio.

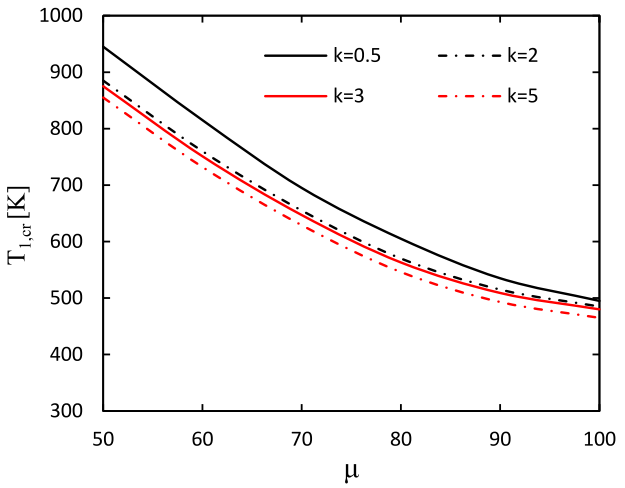

Fig. 10. Dynamic buckling temperature of spherical functionally graded porous shells ($\lambda = 1.7$ and $\xi = 0.1$) for various power-law indices versus slenderness ratio.

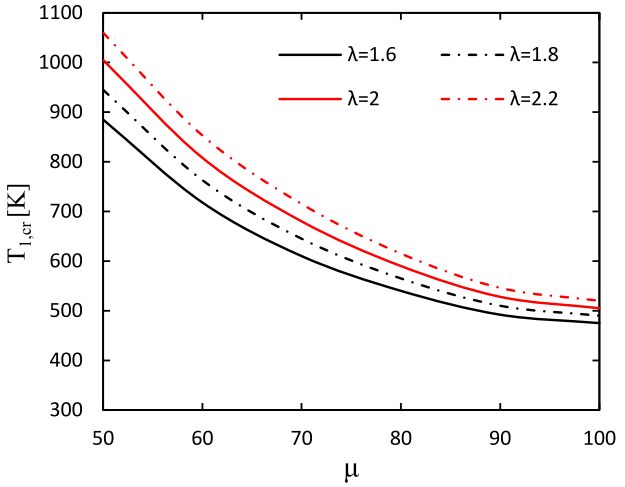

Fig. 11. Dynamic buckling temperature of spherical linearly graded porous shells ($\xi = 0.1$) for various geometrical parameters versus slenderness ratio.

CRediT authorship contribution statement

S. Talebi: Conceptualization, Formal analysis, Funding acquisition, Investigation, Methodology, Software, Validation, Visualization, Writing – original draft, Writing – review & editing. **R. Hedayati:** Investigation, Methodology, Supervision, Visualization, Writing – original draft, Writing – review & editing. **M. Sadighi:** Project administration, Methodology, Supervision, Writing – original draft, Writing – review & editing. **A.R. Ashoori:** Methodology, Supervision, Writing – original draft, Writing – review & editing.

Declaration of competing interest

The authors declare that they have no known competing financial interests or personal relationships that could have appeared to influence the work reported in this paper.

Acknowledgment

The work presented in this paper was supported by a grant from the Iran National Science Foundation.

References

[1] B. Boley, Thermally induced vibrations of beams, J. Japan Soc. Aeronaut. Space Sci. 23 (2) (1956) 179–181.
[2] J. Venkataramana, M. Jana, Thermally forced vibrations of beams, J. Sound Vib. 37 (2) (1974) 291–295.
[3] J. Bruch, S. Adalis, I. Sadek, J. Sloss, Structural control of thermoelastic beams for vibration suppression, J. Therm. Stresses 16 (3) (1993) 249–263.
[4] G. Manolis, D. Beskos, Thermally induced vibrations of beam structures, Comput. Methods Appl. Mech. Engrg. 21 (3) (1980) 337–355.
[5] B. Boley, A. Barber, Dynamic response of beams and plates to rapid heating, ASME J. Appl. Mech. 24 (3) (1957) 413–416.
[6] R. Stroud, J. Mayers, Dynamic response of rapidly heated plate elements, AIAA J. 9 (1) (1971) 76–83.
[7] Y. Nakajo, K. Hayashi, Response of circular plates to thermal impact, J. Sound Vib. 95 (2) (1984) 213–222.
[8] Y. Nakajo, K. Hayashi, Response of simply supported and clamped circular plates to thermal impact, J. Sound Vib. 122 (2) (1988) 347–356.
[9] S. Das, Vibrations of polygonal plates due to thermal shock, J. Sound Vib. 89 (4) (1983) 471–476.
[10] T. Tauchert, Thermal shock of orthotropic rectangular plates, J. Therm. Stresses 12 (2) (1989) 241–258.
[11] J. Chang, J. Wang, T. Tsai, Thermally induced vibrations of thin laminated plates by finite element method, Comput. Struct. 42 (1) (1992) 117–128.
[12] Y. Kiani, M. Eslami, Geometrically non-linear rapid heating of temperature-dependent circular FGM plates, J. Therm. Stresses 37 (12) (2014) 1495–1518.
[13] H. Kraus, Thermally induced vibrations of thin nonshallow spherical shells, AIAA J. 4 (3) (1966) 500–505.
[14] N. Huang, T. Tauchert, Thermally induced vibration of doubly curved cross-ply laminated panels, J. Sound Vib. 154 (3) (1992) 485–494.
[15] N. Huang, T. Tauchert, Large amplitude vibrations of graphite reinforced aluminum cylindrical panels subjected to rapid heating, Compos. Eng. 3 (6) (1993) 557–566.
[16] R. Zoelly, Ueber ein Krichungra Problem und der Kugelschale, (Ph.D. thesis), Switzerland, 1915.
[17] T. von Karman, H. Tsien, The buckling of spherical shells by external pressure, J. Japan Soc. Aeronaut. Space Sci. 7 (2) (1939) 43–50.
[18] W. Wunderlich, U. Albertin, Buckling behaviour of imperfect spherical shells, Int. J. Non-Linear Mech. 37 (4–5) (2002) 589–604.
[19] R. Shahsiah, M. Eslami, Thermal and mechanical instability of an imperfect shallow spherical cap, J. Therm. Stresses 26 (7) (2003) 723–737.
[20] B. Budiansky, R. Roth, Axisymmetric dynamic buckling of clamped shallow spherical caps, NASA Tech. Note 510 (1962) 597–609.
[21] G. Simitses, Axisymmetric dynamic snap-through buckling of shallow spherical caps, AIAA J. 5 (5) (1967) 1019–1021.
[22] R. Ball, J. Burt, Dynamic buckling of shallow spherical shells, J. Appl. Mech. 40 (2) (1973) 411–416.
[23] J. Martinez, J. Stricklin, Dynamic buckling of clamped spherical cap under step pressure loadings, AIAA J. 7 (6) (1969) 1212–1213.
[24] M. Javani, Y. Kiani, M. Eslami, Dynamic snap-through of shallow spherical shells subjected to thermal shock, Int. J. Press. Vessels Pip. 179 (2020) 104028.
[25] R. Alwar, B. Reddy, Dynamic buckling of isotropic and orthotropic shallow spherical cap with circular hole, Int. J. Mech. Sci. 21 (11) (1979) 681–688.
[26] M. Ganapathi, T. Varadan, Dynamic buckling of orthotropic shallow spherical shells, Comput. Struct. 15 (5) (1982) 517–520.
[27] P. Dumir, M. Gandhi, Y. Nath, Axisymmetric static and dynamic buckling of orthotropic shallow spherical caps with flexible supports, Acta Mech. 52 (1–2) (1984) 93–106.
[28] M. Ganapathi, T. Varadan, Dynamic stability characteristics of functionally graded materials shallow spherical shells, Compos. Struct. 79 (3) (2007) 338–343.
[29] T. Prakash, M. Singha, M. Ganapathi, Nonlinear dynamic thermal buckling of functionally graded spherical caps, AIAA J. 45 (2) (2007) 505–508.
[30] M. Sabzikar Boroujerdy, M. Eslami, Axisymmetric snap-through behavior of Piezo-FGM shallow clamped spherical shells under thermo-electro-mechanical loading, Int. J. Press. Vessels Pip. 120–121 (2014) 19–26.
[31] Y. Wang, J. Zu, Large-amplitude vibration of sigmoid functionally graded thin plates with porosities, Thin-Walled Struct. 119 (2017) 911–924.
[32] A. Rezaei, A. Saidi, M. Abrishamdari, M. Pour Mohammadi, Natural frequencies of functionally graded plates with porosities via a simple four variable plate theory: An analytical approach, Thin-Walled Struct. 120 (2017) 366–377.
[33] Y. Wang, Y. Wan, Y. Zhang, Vibrations of longitudinally traveling functionally graded material plates with porosities, Eur. J. Mech. A Solids 66 (2017) 55–68.
[34] Y. Wang, J. Zu, Vibration behaviors of functionally graded rectangular plates with porosities and moving in thermal environment, Aerosp. Sci. Technol. 69 (2017) 550–562.
[35] Y. Wang, Z. Yang, Nonlinear vibrations of moving functionally graded plates containing porosities and contacting with liquid: internal resonance, Nonlinear Dynam. 90 (2017) 1461–1480.
[36] M. Heshmati, F. Daneshmand, A study on the vibrational properties of weight-efficient plates made of material with functionally graded porosity, Compos. Struct. 200 (2018) 229–238.
[37] K Li, D Wu, X Chen, J Cheng, Z Liu, W Gao, M Liu, Isogeometric analysis of functionally graded porous plates reinforced by graphene platelets, Compos. Struct. 204 (2018) 114–130.
[38] A. Zenkour, A quasi-3D refined theory for functionally graded single-layered and sandwich plates with porosities, Compos. Struct. 201 (2018) 38–48.
[39] D. Shahsavari, M. Shahsavari, L. Li, B. Karami, A novel quasi-3D hyperbolic theory for free vibration of FG plates with porosities resting on Winkler/Pasternak/Kerr foundation, Aerosp. Sci. Technol. 72 (2018) 134–149.
[40] D. Bich, D. Dung, L. Hoa, Nonlinear static and dynamic buckling analysis of functionally graded shallow spherical shells including temperature effects, Compos. Struct. 94 (9) (2012) 2952–2960.
[41] Q. Li, D. Wu, X. Chen, L. Liu, Y. Yu, W. Gao, Nonlinear vibration and dynamic buckling analyses of sandwich functionally graded porous plate with graphene platelet reinforcement resting on Winkler–pasternak elastic foundation, Int. J. Mech. Sci. 148 (1) (2018) 596–610.
[42] D. Chen, J. Yang, S. Kitipornchai, Buckling and bending analyses of a novel functionally graded porous plate using Chebyshev-Ritz method, Arch. Civil Mech. Eng. 19 (1) (2019) 157–170.
[43] V. Nam, N. Trung, L. Hoa, Buckling and postbuckling of porous cylindrical shells with functionally graded composite coating under torsion in thermal environment, Thin-Walled Struct. 144 (1) (2019) 106253.
[44] P. Thang, T. Nguyen-Thoi, D. Lee, J. Kang, J. Lee, Elastic buckling and free vibration analyses of porous-cellular plates with uniform and non-uniform porosity distributions, Aerosp. Sci. Technol. 79 (2018) 278–287.
[45] P. Cong, T. Chien, N. Khoa, N. Duc, Nonlinear thermomechanical buckling and post-buckling response of porous FGM plates using Reddy's HSDT, Aerosp. Sci. Technol. 77 (2018) 419–428.
[46] Y.S. Touloukian, Thermophysical Properties of High Temperature Solid Materials, Macmillan, 1967.
[47] J.N. Reddy, C.D. Chin, Thermomechanical analysis of functionally graded cylinders and plates, J. Therm. Stresses 21 (6) (1998) 593–626.